

# Detecting Parts for Action Localization

Nicolas Chesneau

nicolas.chesneau@inria.fr

Grégory Rogez

gregory.rogez@inria.fr

KartEEK Alahari

kartEEK.alahari@inria.fr

Cordelia Schmid

cordelia.schmid@inria.fr

Inria\*

---

## Abstract

In this paper, we propose a new framework for action localization that tracks people in videos and extracts full-body human tubes, i.e., spatio-temporal regions localizing actions, even in the case of occlusions or truncations. This is achieved by training a novel human part detector that scores visible parts while regressing full-body bounding boxes. The core of our method is a convolutional neural network which learns part proposals specific to certain body parts. These are then combined to detect people robustly in each frame. Our tracking algorithm connects the image detections temporally to extract full-body human tubes. We apply our new tube extraction method on the problem of human action localization, on the popular JHMDB dataset, and a very recent challenging dataset DALY (Daily Action Localization in YouTube), showing state-of-the-art results.

## Introduction

Human action recognition in videos is one of the most active fields in computer vision [1, 2, 3]. It offers a broad range of potential applications ranging from surveillance to auto-annotation of movies, TV footage or sport-videos analysis. Significant progress has been made recently with the development of deep learning architectures [4, 5, 6]. Action localization in videos comprises recognizing the action as well as locating where it takes place in the sequence. A popular method for achieving this is to track the person(s) of interest during the sequence, extract image features in the resulting “human tube” i.e., the sequence of bounding boxes framing a person, and recognize the action occurring inside the tube. Such a method performs well when people are fully visible, and when correspondences can be established between tubes extracted from different videos. This hypothesis does not hold for most real-world scenarios, e.g., in YouTube videos, where occlusions and truncations at image boundaries are common and makes action recognition more challenging. State-of-the-art tracking algorithms [7] estimate a bounding box around the visible parts of a person, resulting in non-homogeneous tubes that can cover parts of the human body, the full-body or a mix of both in cases of close-up or moving cameras. For example, in Figure 1, a standard human tube extraction method frames the upper-body of the woman ironing, then the hands

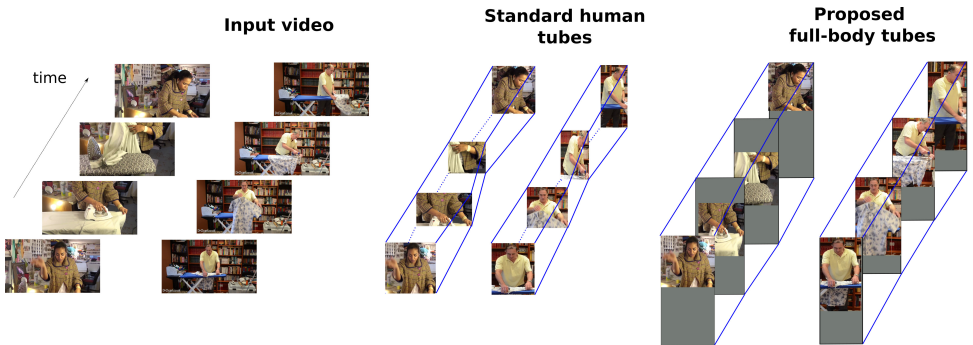


Figure 1: Two example videos from the DALY dataset to illustrate the difference between our human tube extraction and previous methods (a state-of-the-art method [23] is used for illustration here). Note that our tubes (shown on the right) take the occluded parts as well as parts beyond the image boundaries into account.

and arms, and finally the upper-body again. We posit that extracting full-body human tubes, even in case of occlusions or truncations, should help establish better correspondences and extract more discriminative features, improving action localization performance in complex scenarios.

The intuition behind our approach is that a bounding box corresponding to the full human body can often be inferred even if only parts of the person are visible—scene context and body pose constraints (feasible kinematic configurations) help estimate where the occluded or truncated body parts are (see the examples shown in our extracted tubes in Figure 1). To exploit such cues, we propose to train a human part detector that scores the visible parts but also regresses a full-body bounding box. We present a new tracking algorithm that simultaneously tracks several parts of a person-of-interest and combines the corresponding full-body bounding boxes inferred (regressed) from these parts to reliably localize the full-body. We demonstrate that our novel tube extraction approach outperforms state-of-the-art algorithms for action detection and localization [22, 23].

## 2 Related work

Initial attempts for temporal and spatio-temporal action localization are based on a sliding-window scheme and handcrafted descriptors [2, 3, 13, 25]. Other approaches, such as [10, 11], rely on figure-centric models, wherein the person performing the action and their location is detected in some form. In [12], the location of a person is treated as a latent variable when inferring the action performed, while the upper body is explicitly detected and tracked in [10]. Our approach is also based on human detections but is significantly more robust to large variations in pose and appearance, due to our learning-based algorithm. More recently, methods based on action proposals [4, 14, 15, 21, 24] have been employed to reduce the search complexity and improve the quality of tracks, referred to as “tubes”. This paradigm has produced promising results, but these methods generate thousands of proposals even for a short video sequence, and are not scalable to large video datasets. Moreover, they do not take hidden parts and occlusions into account, and are very sensitive to viewpoint changes. In contrast, our method computes one tube for each person in the sequence, taking into account body parts that are occluded or truncated by image boundaries, thereby addressing the problem of amodal completion [10] in the context of action localization.

Recent work has leveraged the success of deep learning for vision tasks in the context of

human action localization [6, 16, 19, 22], by using successful object detectors, like region proposal-based convolutional neural networks [17]. Region-CNNs (R-CNNs) are trained for both appearance and motion cues in these methods to classify region proposals in individual frames. Human tubes are then obtained by combining class-specific detections with either temporal linking based on proximity [6], or with a tracking-by-detection approach [22]. State-of-the-art methods [16, 19] rely on an improved version of R-CNN, e.g., Faster R-CNN [17], trained on appearance and flow. These methods make extensive use of bounding box annotations in every frame for training the network. Although this scheme is accurate for short videos, it is not scalable to long videos with viewpoint changes and close-ups, such as the examples shown in Figure 1. Our method automatically determines the best part to track and infers the global localization of the person from the part alone. The merging step of this inference for each part refines the final bounding box proposed for the frame.

The very recent work in [23] is also related to our approach. It extracts human tubes with a Faster R-CNN based detector. These tubes are then used to localize and detect actions by combining dense trajectories, appearance and motion CNN classifiers. However, this method is also limited to tubes which frame only visible parts of people, and as a result loses spatial correspondences between frames, thus impacting feature extraction. In contrast, our method tracks the entire person during the full sequence, making it robust to partial occlusions, and preserves spatial information for feature extraction and action classification. We establish new state-of-the-art results on the challenging DALY dataset proposed in [23], which consists of 31 hours of YouTube videos, with spatial and temporal annotations for 10 everyday human actions.

## 3 Method: From Parts to Tubes

We propose a new framework for action localization that tracks people in videos and extract full-body humans tubes, even in case of occlusions or truncations. This is achieved by training a novel human part detector that scores visible parts while regressing full-body bounding boxes. Figure 2 shows an overview of our detection architecture that is detailed in Section 3.1. The training phase begins with selection of part proposals that overlap with groundtruth bounding boxes. These part proposals are then assigned a particular class label based on their height-width ratio and location with respect to the bounding box. Finally, a class specific regressor is trained to infer the full-body bounding box from these parts. At test time, given an image, we first generate part proposals which are scored, and then use them to regress full-body bounding boxes, see example in Figure 2. We then merge these bounding boxes using a new tracking algorithm, detailed in Section 3.2. This algorithm simultaneously tracks several parts of a person-of-interest and combines the bounding boxes inferred from these parts to construct a full-body human tube. Two examples are given in Figure 1. Our tube extraction approach is then employed for action localization as detailed in Section 3.3.

### 3.1 Detecting Parts

Inspired by recent advances of deep learning for computer vision problems, we propose a CNN-based human part detector which is end-to-end trainable. Given a database of images annotated with full-body 2D human poses, we first define a set of human parts from this training data. Then, the learning phase trains our detector to: (1) generate relevant human part proposals through a region proposal network (RPN) [17], (2) classify and score them, and (3) regress the corresponding full-body bounding boxes.

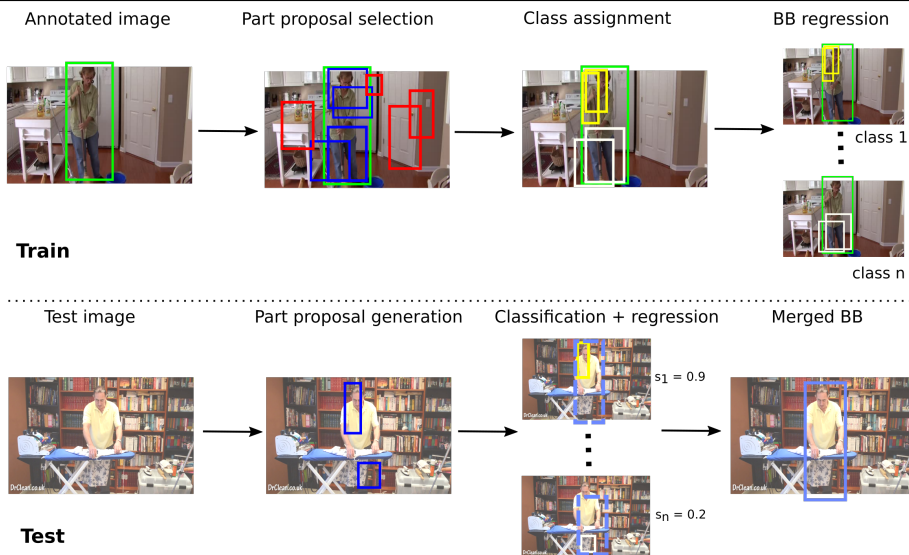


Figure 2: Overview of our part detector. During training, the detector learns to select relevant part proposals in the annotated images. These proposals are assigned a specific class label and employed to regress the target full-body bounding box (BB). At test time, the detector generates part proposals, which are then classified and used to regress full-body bounding boxes. These are merged to estimate the final bounding box (Merged BB).

**Parts definition.** In this paper, a human part is defined as a rectangular region covering a small area of the full-body bounding box. It is represented by its location within the bounding box (e.g., the “upper right” part), an aspect ratio (e.g., a “square” or a “rectangular” part), and a scale. A set of parts is first extracted from the training set using a RPN [14]. The parts must be big enough to contain relevant information and relatively small to ensure that multiple different parts will cover the bounding box. To ensure having small parts, we consider only regions overlapping a groundtruth box with an intersection over union (IoU) score below a certain threshold. Each part is then represented by a four-dimensional vector containing its 2D location with respect to the bounding box center (normalized by bounding box height and width) and its normalized height and width, expressed as percentages of the bounding box height and width. The four values are between 0 and 1. A K-means clustering is finally performed on the set of vectors. The centroids of the resulting  $K$  clusters define our set of part classes. We augment this set of classes with an additional full-body class.

**Parts proposal selection.** As in [14], our architecture uses a RPN to find a set of rectangular candidate regions. During the learning phase, this set is split into positive (blue boxes in Figure 2) and negative proposals (red boxes in Figure 2). We consider a proposal as positive if it is contained in the groundtruth box and has a fixed number of connected body keypoints, with two keypoints being connected if they are directly linked on the human skeleton (e.g., head and shoulders).

**Class-specific regression.** For the class assignment stage, proposals that have a large IoU score with the groundtruth box are labeled as full-body proposals, while others are assigned to the closest part class, which is obtained by choosing the corresponding centroid with the minimum  $\ell_2$ -distance. Note that the groundtruth bounding box is considered as a positive full-body proposal to include at least one positive exemplar for each class. The regression

step then learns to regress the 2D image coordinates of the full-body bounding box. This is done independently for each class to ensure class-specific regression. The goal here is to localize the rest of the body from a single part. In the example in Figure 2, two proposal boxes each are assigned to the classes corresponding to the upper-left area (shown in yellow) and the legs area (in white). The full-body regression target is shown in green. We maintain a fixed ratio between part proposals and full-body exemplars in the training batches.

**Test time.** Our detector first generates relevant part proposals (blue boxes in the lower part of Figure 2). A full-body bounding box is regressed from each of these proposals (dashed boxes in the figure). These regressed boxes corresponding to different part classes can be merged to produce a single full-body bounding box in a frame with a weighted average, where the weights are the classification scores. In Figure 2, the yellow box with a higher score (0.9) has a greater influence than the white box (0.2) on the final merged bounding box. This produces reasonable detections in several cases, but we present a more robust approach which leverages all the candidate boxes for building tubes.

## 3.2 Building full-body tubes

Given the parts detected, and the corresponding regressed bounding boxes for the full body, the next task is to build full-body tubes. We perform this by tracking all the parts detected in each frame, to associate them temporally to their corresponding parts in other frames, and then use them jointly to localize the person(s) performing action. To this end, we extend the tracking algorithm in [22], which is limited to tracking the person as a whole and can not handle challenging cases where the person is occluded, as demonstrated in the experimental results (see Section 4.3).

**Initialization and tracking the first part.** We start by detecting body parts in the entire video sequence, as described in Section 3.1. We find the box  $b^*$  with the highest score among all the part classes, and use it to initialize our tracking algorithm. Let this box be from frame  $t$  in the video, and let  $B^*$  be the corresponding full-body (regressed) bounding box. In frame  $t + 1$ , we perform a sliding window search around the location of the tracked box  $b^*$ , and select the top scoring box. This score is a combination of the generic part detector score (given by the detector in Section 3.1) and an instance-level tracker. The instance-level tracker learns human part appearance in the initialization frame  $t$ , with a linear SVM and features from the last fully-connected layer of our part detector. It is updated every frame with the corresponding chosen box, in order to handle appearance changes over time. The box  $b_{t+1}$  which maximizes the sum of part detector and instance-level scores, is regressed with our part detector into a full-body box  $B_{t+1}$ , and it becomes part of the tube for frame  $t + 1$ .

**Tracking several parts.** Limiting the tracker to a single body type, which may become occluded in some of the frames, is prone to missing the person performing an action. To address this, we detect other parts included into the full-body box  $B_{t+1}$  in frame  $t + 1$ . For example, if the first tracked part is the torso of a person, a second part could be legs detected by our parts detector. Each detected part is then tracked independently in following frames, with the method described above. The regressed full-body boxes of these tracked parts are then combined to produce one full-body box in each frame, with a weighted average of the sum of the part detector and instance-level scores.

## 3.3 Action localization

The final step of our approach is to localize actions from the extracted full-body tubes. We achieve this by representing tubes with features and then learning an SVM for recognizing actions. We use dense trajectories, RGB and Flow CNNs as features. A human tube is



Figure 3: Qualitative results. The visible part of our full-body tubes is shown in blue. For comparison, the tubes of the state-of-the-art method [23] are in red. Here, we show a sample frame from four example videos corresponding to *Cleaning windows*, *Drinking*, *Folding Textile*, and *Ironing* events of DALY.

considered as positive if the temporal intersection over union (IoU) with the annotated frames is above a certain threshold. The temporal IoU is defined as the average per-frame IoU. For this step, our tubes are cropped to frame boundaries to be comparable with groundtruth annotations. For both RGB and Flow CNN, a R-CNN network is trained on the respective dataset (i.e., JHMDB and DALY) as follows: region proposals in a frame whose IoU with our estimated bounding box is above a threshold are labeled as positives for the class of the tube. Action classifiers are learned for each of the features independently and then combined using a late-fusion strategy. These steps are described in detail in Section 4.2.

## 4 Experiments

### 4.1 Datasets

**Test data.** We evaluate our method on two action recognition datasets, namely JHMDB [8] and DALY [23]. JHMDB is a standard action recognition database used in [6, 16, 19, 22, 23]. It is a subset of the larger HMDB51 dataset collected from digitized movies and YouTube videos. It contains 928 videos covering 21 action classes. DALY is a more challenging large-scale action localization dataset consisting of 31 hours of YouTube videos (3.3M frames, 3.6k instances) with spatial and temporal annotations for 10 everyday human actions. Each video lasts between 1 and 20 minutes with an average duration of 3min 45s. We also use the LSP dataset [9] for analyzing our full-body box generation method. LSP contains 2000 pose annotated images of mostly sports people gathered from Flickr.

**Training data.** For training our human part detector, we use the MPII human pose dataset [10]. It covers around 400 actions and contains a wide range of camera viewpoints. The training set consists of around 17k images, with each scene containing at least one person, often occluded or truncated at frame boundaries. As in [23], we compute a groundtruth bounding box for each person by taking the box containing all annotated body keypoints with a fixed additional margin of 20 pixels. To obtain full-body bounding boxes, in cases of occlusions and truncations (where only visible key points are annotated), we employ a nearest neighbor search on the annotated keypoints to complete missing annotations and recover complete full-body 2D poses. As done in [18], we generate a large set (8M) of human 2D poses by projecting 3D poses from the CMU Motion Capture dataset on multiple random camera views. Then, for each incomplete 2D pose in the MPII training set, a search is performed on the annotated 2D joints to estimate the closest match, i.e., full-body 2D pose, that is later employed to estimate a full-body bounding box.

### 4.2 Implementation details

The implementation of our part detector is based on Faster-RCNN [17] with VGG16 layers [20]. The number of classes is set to 21: 20 human parts and the full body class.

**Part detector.** Keypoints are annotated in the MPII dataset we use to train the detector. The connections between joints are defined following the standard human skeleton (e.g.,



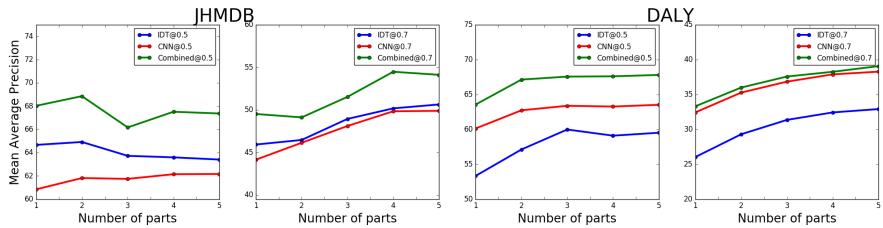


Figure 4: mAP@0.5 and mAP@0.7 results on JHMDB and DALY datasets with respect to the number of parts used for building human tubes.

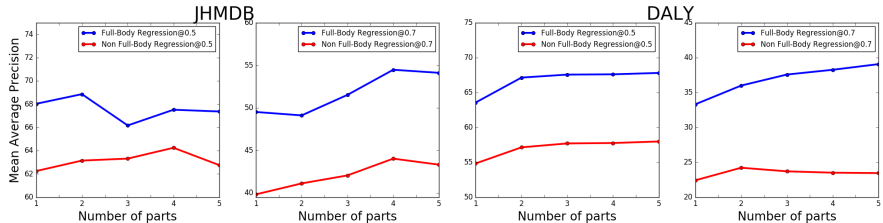


Figure 5: Comparison of our method (trained with full-body boxes) and a variant that only uses visible regions. mAP@0.5 and mAP@0.7 results on JHMDB and DALY datasets with respect to the number of parts used for tube generation are shown.

head connected to shoulders, shoulders to elbows). For the part proposal selection stage, we consider a proposal as positive if it overlaps the groundtruth box and contains exactly three connected body keypoints. We tested with different numbers of keypoints and found that three was an optimum number to maximize human detection rate on DALY (with recall@0.5). For the class assignment stage, proposals with IoU more than 0.55 are labeled as full-body proposals, while those with IoU between 0.1 and 0.55 are assigned to the class of the closest part.

**Optimization.** Initialization of the network is done with ImageNet pretrained weights. The number of iterations is set to 180K, the learning rate to 0.001, the momentum to 0.9, the gamma parameter to 0.1, i.e., the learning rate is divided by 10 at every learning step (@ 100K, 150K, 170K iterations). We use batches of 128 proposals (32 positive and 96 background) and constrain each batch to have 10 times more part proposals than full-body exemplars.

**Human tubes.** For the DALY dataset, tubes are computed using every fifth frame for computational reasons. During the tracking procedure, a box is removed if its combined score (defined in Section 3.2) is less than 1. A new part is added to the tube if it has a detector score of 0.25.

**Action localization.** The dimensions of the four descriptors (HOG, HOF, MBH<sub>x</sub> and MBH<sub>y</sub>) are reduced by a factor of 2 using PCA and a codebook of 256 Gaussians. Appearance and motion CNNs are based on R-CNN architecture proposed in [9]. Five annotated frames per sequence are used as for computing the temporal IoU with our tubes. A human tube is considered as positive if the temporal intersection over union (IoU) with the five annotated frames is above 0.5. During training, the region proposals whose IoU with our estimated bounding box is above 0.5 are labeled as positives for the class of the tube. One linear SVM classifier each is learned independently for the three feature representations (dense trajectory, appearance and motion CNNs). During test time, scores are scaled between 0 and 1 using a sigmoid, and the global score of a tube is the sum of the three SVM scores.

Features	Method	DALY		JHMDB	
		meanAP@0.5	meanAP@0.7	meanAP@0.5	meanAP@0.7
Dense Trajectories	Ours	58.97	31.35	64.91	46.45
	[23]	53.21	21.57	60.11	41.39
Appearance & motion CNNs	Ours	63.51	38.21	61.81	46.12
	[23]	61.12	28.37	64.08	49.22
	[8]	-	-	53.30	-
	[24]	-	-	60.70	-
	[16]	-	-	73.10	-
	[19]	-	-	71.50	-
Combination	Ours	67.79	39.05	68.85	49.10
	[23]	64.56	29.31	65.80	49.54

Table 1: Comparison to the state of the art with mAP@0.5 and mAP@0.7 measures on DALY and JHMDB datasets. We report results for the fully-supervised variant of [23].

### 4.3 Results

In Table 1, our method shows an improvement over [23] on both DALY and JHMDB, of 3.21% and 3.05% respectively for mAP@0.5. A larger gain is obtained with mAP@0.7 on DALY (9.74% for “Combination”), showing that our method is more accurate for action localization in videos. All the results of [23] were obtained directly from the authors. For AP@0.5, per event results emphasize the role of detecting and tracking multiple parts (see Table 2). Compared to [23], we significantly improve the performance for actions such as *Applying make up on lips* with 81.91% (vs 68.18% for [23]), *Brushing teeth* with 68.64% (vs 57.61%). Videos of these actions are often close-up views, where the body is not fully visible during all or part of the sequence. This makes computing feature correspondences between frames more difficult for methods such as [23] which do not estimate the full-body bounding box. The difference between the two methods is even more important for AP@0.7: 49.27% (vs 2.62%) for *Applying make up on lips*, 28.62% (vs 20.58%) for *Brushing teeth*. Our human tubes estimate the position of the full body and infer the location of non-visible parts. This provides a canonical region of support for aggregating local descriptors which belongs to the same parts of the body. Although the method in [16] shows better results on JHMDB, our method has the advantage of being scalable to larger datasets and longer videos. It can also be applied in a weakly-supervised way.

Figures 2 and 3 show a selection of qualitative results. Although Figure 2 shows standing persons, people seated are also well-detected. For example, for the *Playing Harmonica* event in DALY, which contains videos of people sitting (34 examples) and standing (16), we observe a significant improvement: over 1.8% and 31% for AP@0.5 and AP@0.7 respectively. Figure 3 compares our tubes with those extracted by [23], showing that our method better handles close-up views and occlusions.

**Influence of part trackers.** Figure 4 shows the mean average precision of our method when varying the number of parts being tracked when building our tubes. The gain of adding parts is particularly significant with AP@0.7 for JHMDB. For AP@0.5, two-part tracking gives the best results because videos are short and viewpoint changes are limited. For AP@0.7, tracking a maximum of four parts improves average precision significantly. On average, we obtain an mAP of 54.46%, with an improvement of 4.92% over [23]. The results for a few specific actions highlight the effectiveness of our tracking. For example, the *wave* action has an average precision of 32.49% with 1-part tracking, and 49.92% when tracking 4 parts. Videos of this action contain two different points of view: a “full-body” point of view, and a “torso” point of view, making the use of full-body tubes relevant and effective. A



Classes	[23]		Ours	
	AP@0.5	AP@0.7	AP@0.5	AP@0.7
ApplyingMakeUpOnLips	68.18	2.62	81.91	49.27
BrushingTeeth	57.61	20.58	68.64	28.62
CleaningFloor	88.54	72.56	68.13	66.85
CleaningWindows	77.37	35.25	78.13	53.05
Drinking	44.10	13.99	36.77	24.86
FoldingTextile	58.90	35.35	60.77	15.94
Ironing	78.28	39.38	82.52	29.68
Phoning	52.06	25.05	63.41	34.19
PlayingHarmonica	68.36	26.93	70.18	58.12
TakingPhotosOrVideos	52.19	21.36	49.42	29.95
Mean	64.56	29.31	67.79	39.05

Table 2: Per-event results on the DALY dataset of our method and [23]. The results of our method correspond to the one using five parts for human tracking (see Section 3.2).

similar observation can be made with the *climb stairs* action (“full body” and “legs” points of view), with a gain of 8.27% (50.80% with single-part tracking, 59.07% with 4 parts), and also for the *throw* action, with a significant number of upper-body and head videos (18.74% with single-part tracking, 45.90% with 4). On the contrary, the *walk* action shows better results with a single-part tracker (67.56%, compared to 64.59%) because the body of the person walking is fully visible in all the videos, and using the full-body class suffices. On the DALY dataset, a five-part tracker gives the best results. This is partly due to DALY being a much more challenging dataset than JHMDB.

**Influence of fully-body tubes.** Figure 5 compares the performance of part detectors that regress to full-body (including occluded or truncated regions) vs those that regress only to visible regions (i.e., non full-body). Building non full-body tubes decreases the performance, for example, from 68.85 to 63.14 on JHMDB, from 67.79 to 57.97 on DALY for AP@0.5. It confirms our idea that building full-body tubes instead of the standard ones are well-adapted for action localization and classification, and can: (1) establish better feature correspondences, and (2) better exploit techniques such as spatial pyramid matching (SPM) for recognition tasks. Additional experiments show that SPM is more effective with dense tracks when considering our full-body tubes (+3% mAP) vs cropped and mis-aligned tubes from [23] (+1%). In essence, such an “amodal completion” defines a better reference frame for features (spatio-temporal grid is more adapted as person-centric), and results in better performance in the context of action localization.

**Influence of keypoints.** The results in Figure 6(a) highlight the importance of keypoint based proposal generation. We compare our full method, which uses keypoints for selecting parts proposals (refer Section 3.1) with a variant that considers a proposal as positive if its overlap with ground truth is in the range of 0.2 and 0.6, i.e., without using keypoints. The performance of this no-keypoint variant is lower than our full method: 65.87 vs 68.85 on JHMDB, and 67.22 vs 67.79 on DALY.

**Analysis of full-body box generation.** We simulated partially-occluded human poses on the LSP dataset for this analysis. Given a full pose, we successively remove the lowest keypoint in the human pose/skeleton, then the two lowest keypoints, and so on. We then estimate the full-body box with our method for each of these simulated incomplete poses, i.e, the box which frames the full estimated pose. The effectiveness of this estimation is measured by comparing it with the groundtruth box. We do this experiment by removing successively the highest, the left-most, and the right-most keypoints. Results are shown in Figure 6(b). Full-body boxes estimated with 9 out of the 13 keypoints (which corresponds to missing legs for the “lowest” experiment, and missing head and shoulders for the “highest” experiment)

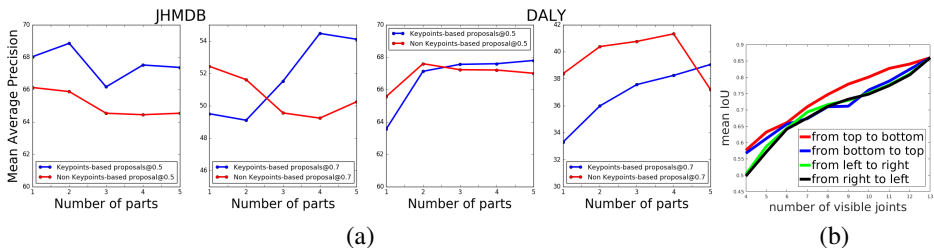


Figure 6: (a) Influence of keypoint based proposal generation. (b) Mean IoU of our full-body box generation method and groundtruth boxes on the LSP dataset, with respect to the number of visible keypoints.

gives a mean IoU over 0.7 with the groundtruth in all the four cases. With only 4 out of 13 keypoints, the IoU remains relatively high (between 0.5 and 0.6).

**Analysis of annotations.** Although our method shows state-of-the-art results on action localization, it suffers from an annotation bias. Our human tubes frame the full body, including hidden parts. For the *Ironing* event in DALY, legs are frequently hidden by ironing boards (see Figure 1 with two examples of DALY videos where the ironing event occurs), and the annotations are focused on visible parts of the body, i.e., the torso and arms. Consequently, the IoUs between our tubes and annotations suffer from the fact that they do not cover the same parts of the actors. To estimate the impact of this annotation bias, we re-annotated the groundtruth bounding boxes in all *Ironing* sequences from DALY taking into account the hidden body parts. We then computed the AP@0.5 and AP@0.7 with dense trajectories and CNNs. With these new annotations, we obtain an average precision of 85.2% (45.55% for AP@0.7), whereas average precision with original annotations is 82.52% (29.68% for AP@0.7). The method in [13] obtains an average precision of 78.28% (39.38% for AP@0.7) with the original annotations. The experiment shows that the classical way of annotating humans in computer vision datasets, i.e., annotating only visible parts, is not ideal to correctly evaluate our full-body tube extractor. However, our results show significant improvements in action localization in a semi-supervised way. Although we train our part detector for people detection, it can be extended to all objects. The main point is to have a training dataset with annotations for the full object, i.e., taking into account hidden parts. Our part detector can also be used with tracking by detection algorithms [19].

## 5 Conclusion

We proposed a novel full-body tube extraction method based on a new body part detector. These detectors are specific to body parts, but regress to full-body bounding boxes, thus localizing the person(s) in a video. Our tube extraction method tracks several human parts through time, handling occlusions, view point changes, and localizes the full body in any of these challenging scenarios. We showed that using our full-body tubes significantly improves action localization compared to methods focusing on tubes built from visible parts only, with state-of-the-art results on the new challenging DALY dataset.

**Acknowledgments.** This work was supported in part by the ERC advanced grant ALLEGRO, the Indo-French project EVEREST funded by CEFIPRA and an Amazon research award. We gratefully acknowledge the support of NVIDIA with the donation of GPUs used for this research.

## References

- [1] M. Andriluka, L. Pishchulin, P. Gehler, and B. Schiele. 2d human pose estimation: New benchmark and state of the art analysis. In *CVPR*, 2014.
- [2] L. Cao, Z. Liu, and T. Huang. Cross-dataset action detection. In *CVPR*, 2010.
- [3] A. Gaidon, Z. Harchaoui, and C. Schmid. Temporal Localization of Actions with Actoms. *IEEE Trans. PAMI*, 2013.
- [4] R. Girshick, J. Donahue, T. Darrell, and J. Malik. Rich feature hierarchies for accurate object detection and semantic segmentation. In *CVPR*, 2014.
- [5] G. Gkioxari and J. Malik. Finding action tubes. In *CVPR*, 2015.
- [6] S. Hare, A. Saffari, and P.H.S. Torr. Struck: Structured output tracking with kernels. In *ICCV*, 2011.
- [7] M. Jain, J. van Gemert, H. Jégou, P. Bouthemy, and C. Snoek. Action localization by tubelets from motion. In *CVPR*, 2014.
- [8] H. Jhuang, J. Gall, S. Zuffi, C. Schmid, and M. J. Black. Towards understanding action recognition. In *ICCV*, 2013.
- [9] S. Johnson and M. Everingham. Clustered pose and nonlinear appearance models for human pose estimation. In *BMVC*, 2010.
- [10] A. Kar, S. Tulsiani, J. Carreira, and J. Malik. Amodal completion and size constancy in natural scenes. *ICCV*, 2015.
- [11] A. Kläser, M. Marszalek, C. Schmid, and A. Zisserman. Human Focused Action Localization in Video. In *International Workshop on Sign, Gesture, and Activity (SGA)*, 2010.
- [12] T. Lan, Y. Wang, and G. Mori. Discriminative figure-centric models for joint action localization and recognition. In *ICCV*, 2011.
- [13] I. Laptev and P. Pérez. Retrieving actions in movies. In *ICCV*, 2007.
- [14] M. Marian Puscas, E. Sangineto, D. Culibrk, and N. Sebe. Unsupervised tube extraction using transductive learning and dense trajectories. In *ICCV*, 2015.
- [15] D. Oneata, J. Revaud, J. Verbeek, and C. Schmid. Spatio-Temporal Object Detection Proposals. In *ECCV*, 2014.
- [16] X. Peng and C. Schmid. Multi-region two-stream R-CNN for action detection. In *ECCV*, 2016.
- [17] S. Ren, K. He, R. Girshick, and J. Sun. Faster R-CNN: towards real-time object detection with region proposal networks. In *NIPS*, 2015.
- [18] G. Rogez, P. Weinzaepfel, and C. Schmid. LCR-Net: Localization-Classification-Regression for Human Pose. In *CVPR*, 2017.

- 
- [19] S. Saha, G. Singh, M. Sapienza, P. Torr, and F. Cuzzolin. Deep learning for detecting multiple space-time action tubes in videos. In *BMVC*, 2016.
- [20] K. Simonyan and A. Zisserman. Very deep convolutional networks for large-scale image recognition. *ICLR*, 2014.
- [21] J. van Gemert, M. Jain, E. Gati, and C. Snoek. APT: Action localization proposals from dense trajectories. In *BMVC*, 2015.
- [22] P. Weinzaepfel, Z. Harchaoui, and C. Schmid. Learning to track for spatio-temporal action localization. In *ICCV*, 2015.
- [23] P. Weinzaepfel, X. Martin, and C. Schmid. Human action localization with sparse spatial supervision. *arXiv*, abs/1605.05197, 2016.
- [24] G. Yu and J. Yuan. Fast action proposals for human action detection and search. In *CVPR*, 2015.
- [25] J. Yuan, Z. Liu, and Y. Wu. Discriminative subvolume search for efficient action detection. In *CVPR*, 2009.